PCCP

PAPER

View Article Online
View Journal | View Issue

Check for updates

Cite this: *Phys. Chem. Chem. Phys.*, 2018, **20**, 12642

$CB_3E_2^q$ ($q = \pm1$): a family of "hyparene" analogues with a planar pentacoordinate carbon†

Ping Liu,*[a] Jian-Hong Bian,[b] Qiang Wang,[a] Fang Huang,[c] Debao Li[a] and Yan-Bo Wu*[ab]

Received 22nd February 2018, Accepted 6th April 2018

DOI: 10.1039/c8cp01193a

rsc.li/pccp

A CB_3 moiety extracted from the building units of milestone "hyparenes" (families of species with a planar pentacoordinate carbon (ppC)) was found to be a more basic building block, which can be employed to design a family of "hyparene" analogues $CB_3E_2^q$ ($q = \pm1$) also with a ppC. The majority of main group elements can feasibly serve as the E atom. Despite the number of valence electrons, the ppC atoms in the $CB_3E_2^q$ ($q = \pm1$) species were involved in three delocalized σ orbitals and a delocalized π orbital, so the carbon atom obeys the octet rule. The NICS studies indicated that these ppC structures are σ and π double aromatic. Given that most of them are less favourable in energy than their boron-centered isomers, it is remarkable that the global minimum of $CB_3Mg_2^-$ adopts the ppC arrangement. Such a ppC structure is also kinetically stable. Compared to previously reported anionic ppC global minima, $CB_3Mg_2^-$ does not contain hyper toxic beryllium and thus is much more attractive to our experimental colleagues for realizing the ppC species using negative ion photoelectron detachment spectroscopy.

Introduction

As an extension to non-classical planar tetracoordinate carbon (ptC),[1] planar pentacoordinate and hexacoordinate carbon (ppC and phC) have intrigued chemists for nearly two decades since the Schleyer group proposed the milestone CB_6^{2-} and "hyparenes" in 2000–2001.[2] In comparison with classical bonding for carbon, ptC violates the arrangement of four bonded atoms (planar tetragon *versus* tetrahedron), while ppC and phC further violate the maximum number of bonded atoms (five and six *versus* four).[3] The successful design of ppC and phC species rapidly initiated the extension of the number of planar coordination to higher values and the central planar hypercoordinate atom from carbon to other main group elements or even transition metals.

Notably, photoelectron spectroscopy (PES) played a crucial role in the realization of species with planar hypercoordination. To be detected by PES, it is better that a desired structure is an anionic global energy minimum with no more than three different elements. The examples include the ptC species CAl_4^-,[4] $NaCAl_4^-$,[5] CAl_3Si^-, and CAl_3Ge^-,[6] as well as the transition metal-centered boron wheels[7] CoB_8^-, MB_9^- (M = Ru, Rh and Ir),[7b,7c] NbB_{10}^-, and TaB_{10}^-.[7d] However, as the pivotal intermediate between ptC and a planar hypercoordinate heteroatom or transition metal (phX/TM), the ppC and phC species are still unknown experimentally.

Since no phC global minimum has been reported, it is not curious that phC cannot be realized experimentally. In contrast, the number of theoretically verified ppC global minima is as many as thirty-nine, in which that of a perfect ppC structure is thirty,[3,8] including CAl_5^+,[8a] CAl_4Ga^+,[8b] CAl_4Be, $CAl_3Be_2^-$,[8c] $CAl_2Be_3^{2-}$, $LiCAl_2Be_3^-$,[8d] CBe_5Al^-, CBe_5Ga^-,[8e] $CBe_5Li_n^{n-4}$ (n = 1–5),[8f] $CBe_5H_n^{n-4}$ (n = 2, 3),[8g] $CBe_5Au_n^{n-4}$ (n = 2–5),[8h] $CBe_5E_5^+$ (E = F, Na and K),[8i] CB_3AlMg,[8j] CAl_4TiF_2, and CAl_4TMX_2 (TM = Zr, and Hf, X = F, Cl, Br, I and Cp).[8k] Such a number is much larger than that of the reported ptC, phX, or phTM global minima. Nevertheless, the majority of them are neutral or cationic, which is not suitable for PES, while the limited anionic ppC global minima[8i] all have hypertoxic beryllium, which greatly decreases the enthusiasm of our experimental colleagues and thus deters the corresponding ppC species from being realized experimentally. Therefore, on top of the common requirements mentioned above, "beryllium-free" is also strongly desired for the PES detection of ppC species.

In this work, our attention was paid to the milestone "hyparenes" (families of molecules containing ppC) proposed

[a] State Key Laboratory of Coal Conversion, Institute of Coal Chemistry, Chinese Academy of Sciences, 27 South Taoyuan Road, Taiyuan, Shanxi, 030001, China. E-mail: pingliu@sxicc.ac.cn

[b] Key Laboratory of Materials for Energy Conversion and Storage of Shanxi Province, Institute of Molecular Science, Shanxi University, 92 Wucheng Road, Taiyuan, Shanxi, 030006, China. E-mail: wyb@sxu.edu.cn

[c] College of Chemistry, Chemical Engineering and Materials Science, Shandong Normal University, 88 East Culture Road, Jinan, Shandong, 250014, China

† Electronic supplementary information (ESI) available: Pictures and relative free energies of $CB_3E_2^q$ species not shown in the text, the full set of NBO results, and the Cartesian coordinates of structures studied in this work. See DOI: 10.1039/c8cp01193a

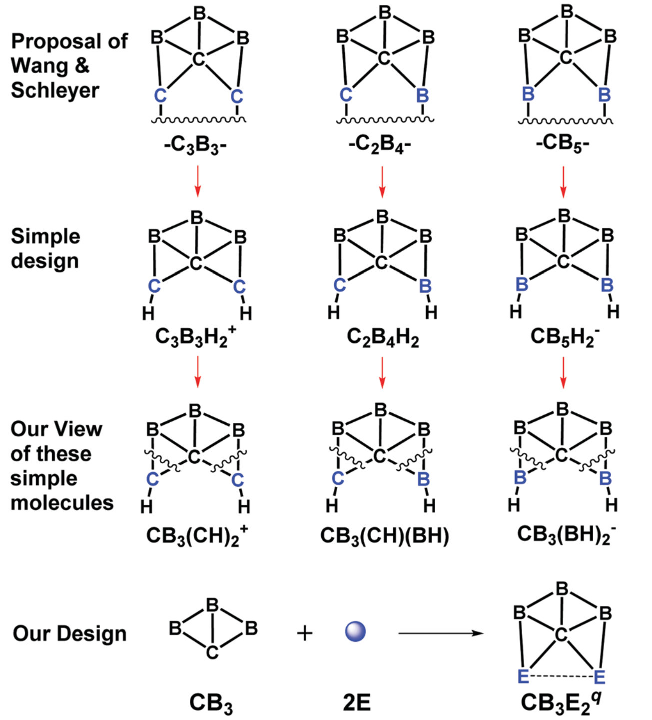

Scheme 1 Relationship between hyparenes and the species designed by us.

by Wang and Schleyer,[2b] hoping that the proper elaboration on hyparenes can match the requirements. Hyparenes were designed by substituting –(CH)$_3$– subunits in aromatic or even anti-aromatic hydrocarbons with the ppC units –C_3B_3–, –C_2B_4–, and –CB_5– (first row of Scheme 1), which can contribute two, one, and zero π electrons, respectively, to the parent system. The simplest molecules constructed by these three units were C_{2v} $C_3B_3H_2^+$, C_s $C_2B_4H_2$, and C_{2v} $CB_5H_2^-$ (second row of Scheme 1), respectively. In our alternative view, hyparenes can be obtained by substituting two H atoms in one of these three species with a hydrocarbon fragment. Indeed, such a perspective can be intensified as follows: a CB_3 moiety can be extracted from hyparene building blocks and the above simplest structures can be seen as $CB_3(CH)_2^+$, CB_3(CH)(BH), and $CB_3(BH)_2^-$, respectively (third row of Scheme 1). Here, if two XH (X = C or B) moieties can be substituted by other atoms (E), CB_3 may be a more basic building unit for the design of borocarbon species with a ppC (fourth row of Scheme 1).

Previously, we have proposed and demonstrated that the thermodynamic stability of species with non-classical carbon bonding can be improved when the covalent character of carbon–ligand bonding is properly weakened.[8d,8g,9] If such an empirical rule is valid in the current system, through adjusting the "E" atoms, it is possible to achieve the desired beryllium-free anionic ppC global minimum with no more than three different elements. In the following, we will show that CB_3^q ($q = \pm1$) themselves are global minima and the majority of the main group elements can feasibly bind the CB_3 unit at the bridging position of the C–B edges, leading to $CB_3E_2^q$ ($q = \pm1$), a family of hyparene analogues with a ppC, in which $CB_3Mg_2^-$ meets all of the above requirements.

Results and discussion

Geometries and electronic structures of CB_3^q ($q = \pm1$)

Our design starts from the basic unit CB_3. Since it has an odd number (21) of electrons, it is desirable to remove or add an electron to achieve species with an even number of electrons, leading to the CB_3^+ and CB_3^- ions, respectively. Using the stochastic search algorithm,[10] we explored the potential energy surfaces of CB_3^+ and CB_3^-, whose global minima were both found to adopt the rhombic C_{2v} structure (see **1a** and **2a** in Fig. 1). At the final ($E_{CCSD(T)} + G_{B3LYP}$)/BS1 level (see the Computational Method section for details), they are 31.3 and 16.1 kcal mol^{-1} lower in energy than their second lowest isomers, respectively. The ground states of CB_3^+ and CB_3^- are closed-shell singlet and open-shell triplet, respectively. Nevertheless, the results of thermodynamic stability revealed that CB_3 is a very rigid unit both as anion and as cation.

To understand the bonding in **1a** and **2a**, we performed orbital analysis. The adaptive natural density partitioning (AdNDP)[11]

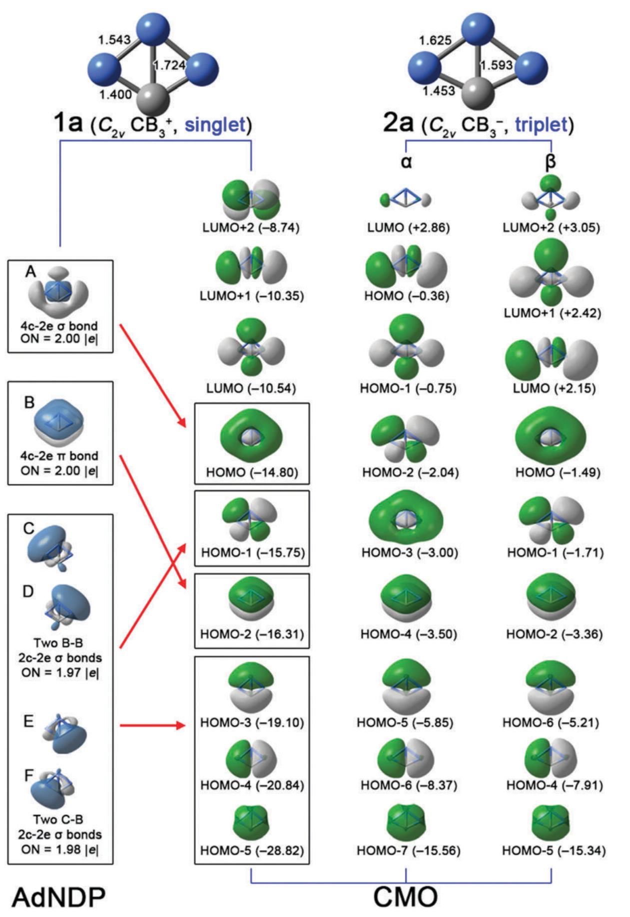

Fig. 1 Optimized structures of **1a** and **2a** at the B3LYP/BS1 level (with necessary bond lengths (in Å) and point groups) and their orbital analysis results. The carbon and boron atoms are shown as grey and blue balls, respectively, and two phases of AdNDP orbitals and CMOs are given in blue/white and green/white, respectively.

View Article Online

procedure is available only for the occupied orbitals of the closed-shell system, so it is just applied to **1a**. As shown in Fig. 1, in six pairs of valence electrons of **1a**, four of them form the localized B–B or C–B two-center two-electron (2c–2e) bonds with occupation numbers (ONs) of 1.97–1.98 |e| (C–F). The remaining two pairs of electrons form a four-center two-electron (4c–2e) σ bond and a 4c–2e π bond, both with ONs of 2.00 |e| (A and B). Fig. 1 also shows the canonical molecular orbitals (CMOs) LUMO and LUMO+1, which mainly come from the vacuum p orbitals of boron atoms. Their orbital energies are very close, being −10.54 and −10.35 eV, respectively. If two electrons are introduced to **1a**, it can be expected that both orbitals will be singly occupied, *i.e.* **2a** should be an open-shell triplet rather closed-shell singlet species, which is consistent with the above results. As shown in Fig. 1, the counterparts of the doubly occupied valence orbitals of **2a** are found in the occupied orbitals of **1a**, while those of the singly occupied orbitals in **2a** are just the LUMO and LUMO+1 in **1a**.

Designing the ppC species $CB_3E_2^q$ ($q = \pm 1$)

The above results suggest that rhombic CB_3 should be a very rigid unit because the geometries of the global minima CB_3^q are not obviously varied when the values of q vary. Therefore, it is reasonable to consider $C_3B_3H_2^+$, $C_3B_3H_2$, and $CB_5H_2^-$ as $CB_3(CH)_2^+$, $CB_3(CH)(BH)$, and $CB_3(BH)_2^-$, respectively. In this work, we tried to substitute two XH (X = B or C) moieties in these species with two E atoms, hoping to achieve new ppC species, especially those of global energy minima.

We searched for the proper E atoms in the periodic table (except for heavy alkali/alkali earth metals, rare earth metals, and noble gases). As shown in Fig. 2, for $CB_3E_2^-$, the feasible E atom can be found in groups 1, 2, and 13–15 (see the elements in yellow and orange regions), while for $CB_3E_2^+$, it can be found in groups 2 and 13–16 (see the elements in orange and pink regions). Indeed, we were somewhat surprised by the results because the majority of main group elements could be employed for designing ppC species.

The optimized structures of $CB_3Li_2^-$ (**3a**) and $CB_3E_2^{+/-}$ (E = Mg–S, **4a–12a**) are shown representatively in Fig. 3. Those of other species are shown in Fig. S1 and S2 in the ESI.† As the figures show, for $CB_3E_2^-$ (E = Be, Mg, and Ca) and $CB_3Al_2^+$, their B_3E_2 peripherals form a closed ring, which leads to a size-matching

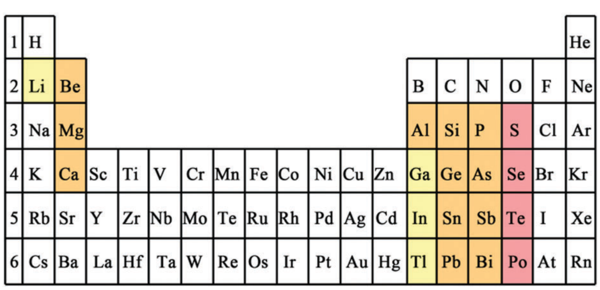

Fig. 2 Distribution of feasible E atoms in the periodic table. Elements in yellow, pink, and orange regions are feasible for $CB_3E_2^-$, $CB_3E_2^+$, as well as both $CB_3E_2^-$ and $CB_3E_2^+$, respectively.

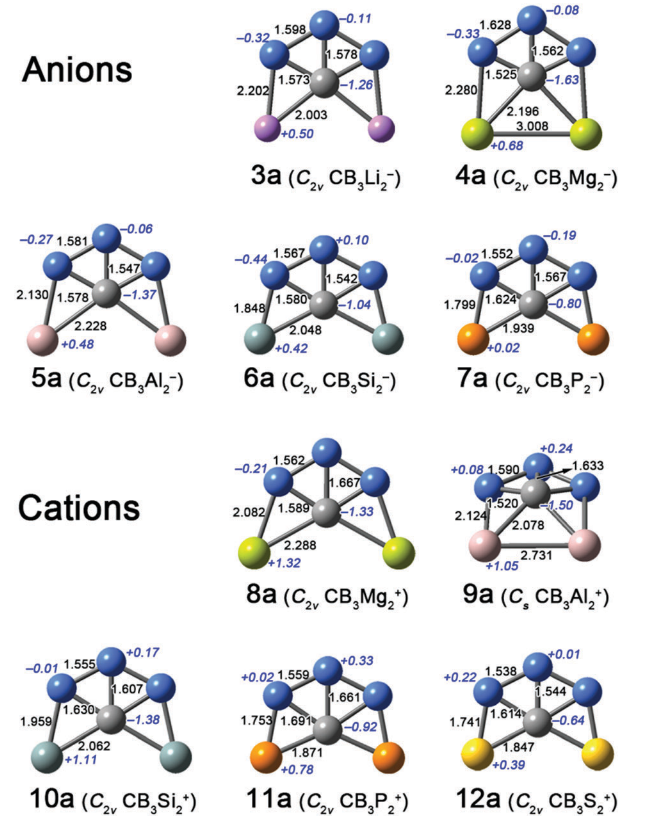

Fig. 3 The representatives of optimized ppC structures of $CB_3E_2^+$ and $CB_3E_2^-$ (E = Li and the third row elements) with necessary bond lengths (in Å) and point groups. The NBO charges are given in italic blue.

issue between carbon and the B_3E_2 ring. As a result, only $CB_3Mg_2^-$ and $CB_3Ca_2^-$ (see **4a** and **14a** in Fig. 3 and Fig. S1 (ESI†), respectively) adopt the planar structure, suggesting a good fit between carbon and the B_3Mg_2/B_3Ca_2 ring. The carbon-centered structures of $CB_3E_2^+$ (E = Ga, In, and Tl) are not minima, so they are not considered. In contrast, there was an indentation between two E atoms in other species, which makes it possible for B_3E_2 peripherals to have a flexible space to well-accommodate the carbon atom in the same plane, so these species all adopt the planar C_{2v} structure. Note that the C–B and C–E distances in all planar species are in the range of or only a little longer than the C–B or C–E single bond lengths,[12] so the carbon atoms in these planar structures can be considered as ppCs.

Electronic structures of $CB_3E_2^q$ ($q = \pm 1$)

To better understand these structures, we performed AdNDP analysis on **3a–12a** and the results are given in Fig. 4. **3a** can be formed from a CB_3^+ cation and two Li^- anions. As displayed in Fig. 1 and 4, of six AdNDP-generated orbitals of CB_3^+, three of them can be found in **3a**, including two B–B 2c–2e σ bonds and a 4c–2e π bond. Nevertheless, the electrons in the remaining three orbitals, including two C–B 2c–2e σ bonds and a 4c–2e σ bond, participate in new bonding orbitals in **3a**, involving two B–Li 2c–2e σ bonds and three CB_3 4c–2e σ bonds. Therefore, **3a** is a 16 valence electron (ve) species. Though 3a does not meet

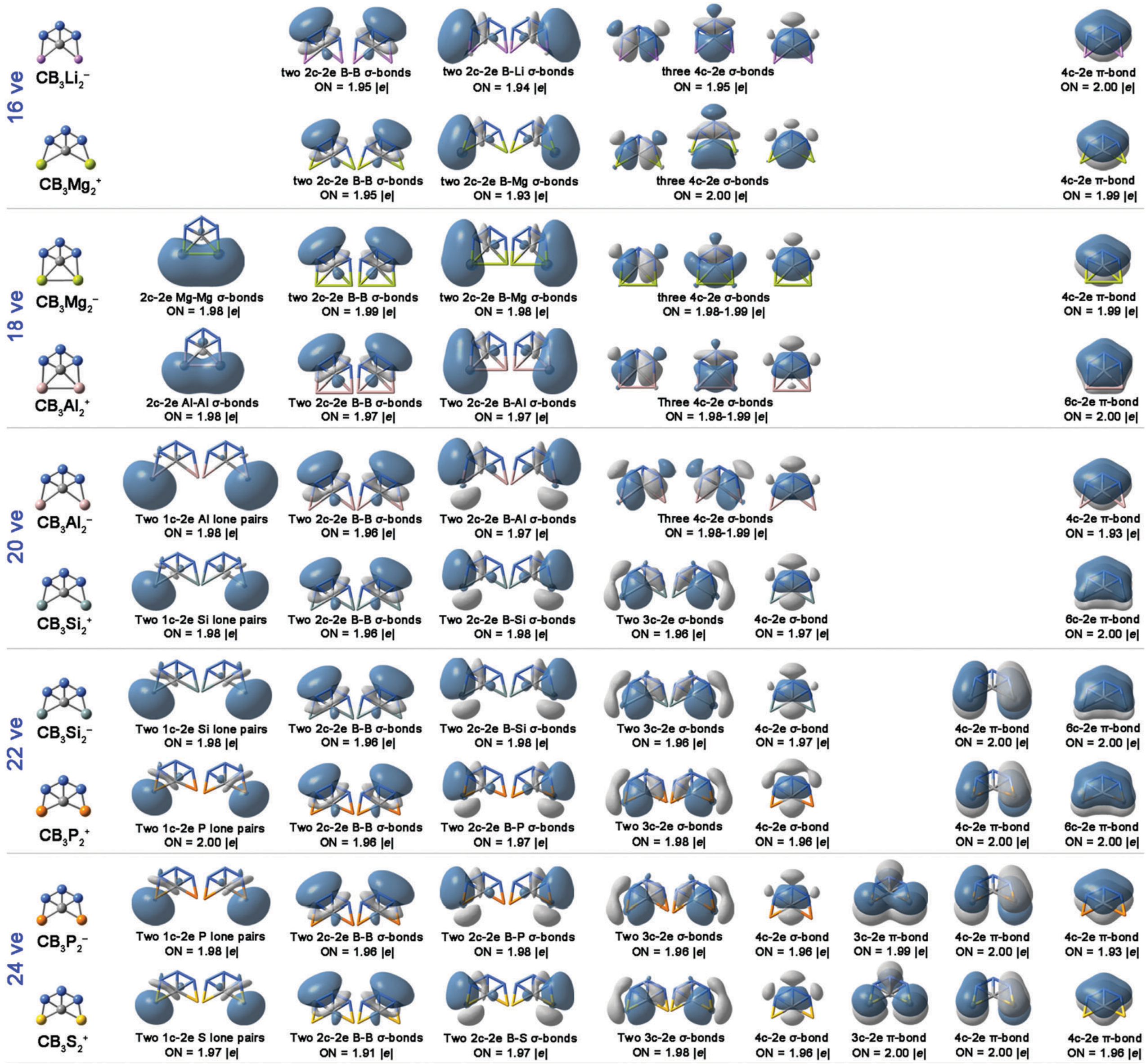

Fig. 4 AdNDP view of chemical bonding in representative species designed in this work. The planar structure of $CB_3Al_2^+$ is employed for easy analysis.

the 18 electron rule, the number of valence orbitals around the central carbon atom is four, so the bonding of carbon obeys the octet rule, which could be a reason why Li is a feasible E atom. $CB_3Mg_2^+$ (**8a**) is isoelectronic to **3a**, so it has similar bonding orbitals to those of **3a**.

In comparison with the 16 ve species **3a** and **8a**, $CB_3Mg_2^-$ (**4a**) and $CB_3Al_2^+$ (**9a**) have 18 ve, which is generally considered to be optimal. As shown in Fig. 4, two more electrons in **4a** and **9a** form a Mg–Mg or Al–Al 2c–2e σ bond, which leads to the formation of a closed B_3Mg_2 or B_3Al_2 ring in **4a** and **9a**. Though such a ring structure slightly influences the shape of orbitals concerning carbon atoms, the number of orbitals around carbon is still four, thus the octet rule is not violated. Instead of an E–E 2c–2e bond in **4a** and **9a**, two 1c–2e lone pairs are found in the 20 ve species $CB_3Al_2^-$ (**5a**) and $CB_3Si_2^+$ (**10a**). Such lone pairs are also found in the 22 ve species $CB_3Si_2^-$ (**6a**) and $CB_3P_2^+$ (**11a**), as well as the 24 ve species $CB_3P_2^-$ (**7a**) and $CB_3S_2^+$ (**12a**). Since there is no orbital describing the E–E bonding in the 20, 22, and 24 ve molecules, the B_3E_2 rings in these species are not closed. Compared to the 20 ve species, two more electrons in the 22 ve species **6a** and **11a** fill into a 4c–2e π bond, which involves two E atoms and two shoulder B atoms but does not involve C and peak B atoms. Similarly, in the 24 ve species **7a** and **12a**, two additional electrons fill into a 3c–2e π bond, which involves two E atoms and a peak B atom but does not involve C and shoulder B atoms. As shown in Fig. 4, the orbital shape suggests that the newly emerged 4c–2e and 3c–2e π bonds mainly originate from the p_z lone pairs of E atoms, which play the role of compensating the π electrons to electron deficient boron atoms. Therefore, such π orbitals do not involve C atoms and the number of orbitals concerning ppC is four, meeting the octet rule as well.

We also performed the natural bond orbital (NBO)[13] analysis to get further insight into the bonding. As shown in Table 1, the total Wiberg bond indices (WBIs) of carbon atoms in **3a–12a** range from 3.36 to 3.98, suggesting that the octet rule is not violated, which is consistent with the orbital analysis. Though the total WBI values for E atoms generally increase with the electronegativity of E atoms, the values for the 20 ve species **5a** and **10a** are smaller than those for the 18 ve species **4a** and **9a** and the 24 ve species **12a** are smaller than those for the 22 ve species **11a**. Such a result is in accordance with the orbital analysis: the valence electrons of **5a** and **10a** form lone pairs, while the S atoms in **12a** show divalency. The WBI_{C-B} values range from 0.68 to 1.07, indicating the significant C–B covalent bonding. Interestingly, for E = Li, Mg, and Al, the WBI_{C-E} values range from 0.13 to 0.24, suggesting rather weak C–E covalent bonding. Such results meet our strategy that the thermodynamic stability can be improved when the covalent characteristic of carbon–ligand interactions is properly weakened. Specifically, we speculate that the 18 ve species **4a** and **9a** may possess good thermodynamic stability.

Aromaticity

The orbital analyses also suggest that there are three delocalized σ orbitals and a delocalized π orbital in the species shown in Fig. 3, so these species may be aromatic. To access the aromaticity, the nucleus-independent chemical shifts (NICSs)[14] were calculated at the B3LYP/BS1 level. The σ-aromaticity was accessed by the in-plane NICS(0) values at the centers of CBB and CBE triangles, while the π-aromaticity was evaluated by the NICS(1) values at 1 Å above the centers of the CBB and CBE triangles as well as above carbon atoms. As shown in Table 1, most of the NICS(0) values are negative, showing that these ppC species are σ-aromatic. The obvious positive NICS(0) values can be found at the center of the CBE triangles of the 20 ve species **5a** and **10a**, which may be due to the influence of their dispersive valence lone pairs. In contrast, all of the NICS(1) values are negative despite the number of π orbitals, revealing that all these species are π-aromatic. Such a result proves again that the 4c–2e and 3c–2e π orbitals mainly originate from the p lone pairs of E atoms, so that they contribute little to the π electron delocalization of these molecules. Taken together, **3a–12a** should be σ and π double aromatic species.[15] It is interesting that the largest negative NICS(1) values can be found in the 18 ve species **4a**.

Planar pentacoordinate boron (ppB) counterparts

Considering the previous common view that boron is more competitive for the planar hypercoordinate positions than carbon, we also studied the structures where two E atoms are attached to the opposite side of a CB_3 rhombus, leading to boron-centered isomers. The counterparts of **3a–12a** are given in Fig. 5, while those of other ppC structures are given in Fig. S1 and S2 in the ESI.† As the figures show, a CB_2E_2 ring can also be found for the boron-centered structures $CB_3E_2^-$ (E = Be, Mg and Ca) and $CB_3Al_2^+$. Due to the size-mismatch, the corresponding boron-centered structures are not planar. The B-centered structures for $CB_3E_2^+$ (E = Ga, In and Tl) are not minima as well, so they are not considered. In contrast, other boron-centered structures have planar structures with C_{2v} point groups and a ppB.

Stability consideration

The thermodynamic stability is very important for the experimental viability of species with non-classical bonding. In this work, we examined the thermodynamic stability of ppC structures in two steps. In the first step, we calculated the relative energies of boron-centered isomers (using the carbon-centered isomers as the references). In most cases, the boron-centered isomers are lower in energy compared to the carbon-centered structures, *i.e.* the corresponding ppC structures are not the global minima, so they are hard to realize experimentally. In addition, though the boron-centered structure of $CB_3Al_2^+$ are higher in energy than the carbon-centered structure (**9a**), the latter is not planar, and it is also not considered in the following. In contrast, the energy of the boron-centered isomer for $CB_3Mg_2^-$ (**4b**) is 7.5 kcal mol^{-1} higher than that of the ppC isomer (**4a**). Thus, in the second step, the $CB_3Mg_2^-$ potential energy surface was extensively explored. At the $(E_{CCSD(T)} + G_{B3LYP})$/BS1 level, **4a** and **4b** are global minima and the fourth lowest isomers, respectively. The second and third lowest isomers (see **4c** and **4d** in Fig. S3, ESI†) locate 2.7 and 4.3 kcal mol^{-1}, respectively, higher than **4a**.

The kinetic stability is equally important for the experimental viability of small clusters. In the present work, the kinetic

Table 1 Wiberg bond indices (WBIs) of C, E, C–E, E–E, C–B_t, and C–B_s (B_t and B_s denote the boron atoms located at top and shoulder positions, respectively); NICS(0) and NICS(1) values are calculated for the points at the centers of CBB/CBE triangles and 1 Å above these two points as well as above the C atom

	WBI						NICS(0)		NICS(1)		
	C	E	C–E	E–E	C–B_t	C–B_s	CBB	CBE	C	CBB	CBE
3a	3.47	0.89	0.18		1.05	1.03	−6.2	−0.6	−6.8	−12.0	−2.8
4a	3.37	1.56	0.14	0.64	1.04	1.03	−16.7	−2.1	−25.5	−20.9	−11.5
5a	3.42	1.02	0.21		1.05	0.98	−11.8	+10.0	−19.2	−13.6	−3.8
6a	3.68	2.35	0.62		0.93	0.89	−7.6	−19.8	−7.7	−4.5	−8.5
7a	3.88	2.53	0.66		0.96	0.80	−36.5	−33.5	−16.5	−11.2	−10.2
8a	3.36	1.02	0.13		0.94	1.07	−11.4	+4.3	−9.6	−14.1	−3.0
9a	3.37	1.64	0.24	0.48	0.85	1.02	−20.7	−11.7	−14.5	−10.0	−4.2
10a	3.45	1.44	0.41		0.90	0.87	−7.0	+10.1	−19.4	−12.2	−7.2
11a	3.80	2.81	0.83		0.78	0.71	−4.3	−26.4	−12.3	−6.5	−12.0
12a	3.98	2.44	0.79		1.03	0.68	−37.8	−32.7	−13.6	−11.0	−6.7

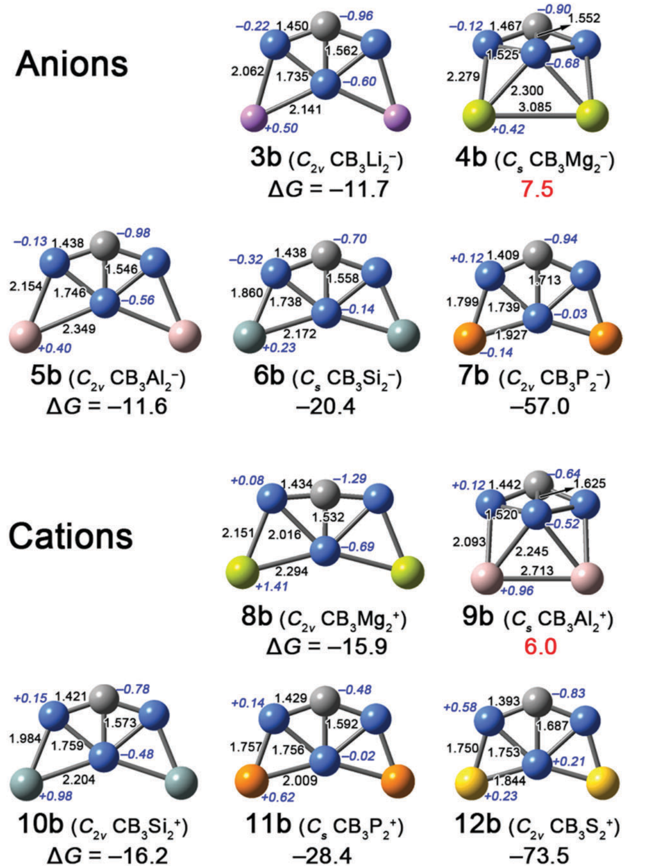

Fig. 5 Optimized structures of the ppB isomers of $CB_3E_2^+$ and $CB_3E_2^-$ (E = Li, and the third row elements) with necessary bond lengths (in Å) and point groups. The NBO charges are given in italic blue and the free energies relative to ppC isomers (Δ*G*) are given in kcal mol^{-1}.

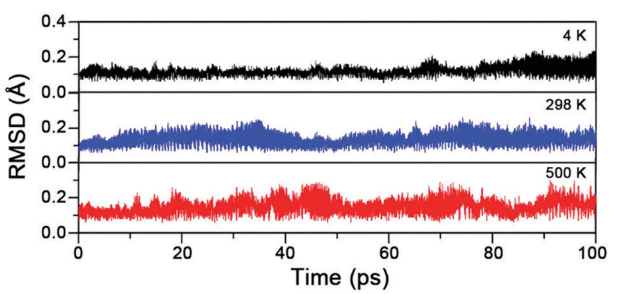

Fig. 6 RMSD *versus* simulation time in the BOMD simulations of **4a** at 4, 298, and 500 K, respectively.

stability of global minimum **4a** was studied using Born-Oppenheimer molecular dynamic (BOMD)[16] simulations at 4, 298, and 500 K and at the B3LYP/6-31G(d) level. The structural evolution during the simulation was described by root-mean-square deviation (RMSD, in Å) of the structures relative to the B3LYP/6-31G(d)-optimized structure. As shown in Fig. 6, at three different temperatures, the RMSD plots of **4a** do not show an upward jump and the fluctuations of RMSD values are relatively small, which suggest **4a** is kinetically stable at least up to 500 K.

Being an anion containing only three elements, the kinetically stable global energy minimum **4a** is suitable for generation in the gas phase followed by detection using PES. Compared to previous "suitable" candidates, **4a** does not contain the toxic beryllium atom, so it would be much more attractive to our experimental colleagues for the realization of species with a ppC.

Conclusions

We found a CB_3 subunit in hyparene building blocks and proved that it was rather rigid upon attaching other atoms. Using CB_3 as the basic structure, we computationally designed a family of species $CB_3E_2^q$ ($q = \pm1$) with a ppC, where most of the main group elements were attested to be feasible E atoms. In spite of the number of total valence electrons, the ppC atoms in these species were involved in four valence orbitals, so the octet rule is not violated, which can be identified by the total Wiber bond index values under 4.00. All these ppC species are σ and π double aromatic in nature. Though most of the ppC structures are less favourable in energy than their boron-centered isomers, the $CB_3Mg_2^-$ ppC structure was verified to be the global energy minimum with good kinetic stability. Different from previously reported anionic global minima with a ppC, $CB_3Mg_2^-$ does not contain the hyper-toxic beryllium atom, which makes it a good target for the experimental realization of a perfect ppC structure.

Computational methods

The structures designed in this work were optimized and characterized to be true minima by frequency analysis calculations at the B3LYP/BSI level, where BSI denotes a mixed basis set, aug-cc-pVTZ for Li–Se and aug-cc-pVTZ-PP for heavier elements. The B3LYP/BS1 results were calibrated using the double hybrid functional at the B2PLYP-D/BSI level. Natural bond orbital (NBO)[13] analysis and nucleus-independent chemical shift (NICS)[14] calculations were performed at the B3LYP/BSI level. In order to further understand the chemical bonding pattern of these structures, adaptive natural density partitioning (AdNDP)[11] analyses were carried out for the species shown in Fig. 1 and 3 at the B3LYP/6-31G level. The relative energies between the ppC structures and their boron-centered isomers were compared by single point energy calculations at the CCSD(T)/BS1 level and corrected using B3LYP/BSI Gibbs free energies, which was abbreviated as ($E_{CCSD(T)} + G_{B3LYP}$)/BS1. The searches for the global minima of CB_3^+, CB_3^-, and $CB_3Mg_2^-$ were carried out by exploring potential energy surfaces using the stochastic search algorithms.[10] The initially generated structures were optimized at the B3LYP/6-31G(d) level. Then, twenty lowest energy minima were re-optimized at the B3LYP/BS1 level. Finally, the energies of the lowest ten isomers selected from re-optimizations were compared at the ($E_{CCSD(T)} + G_{B3LYP}$)/BS1 level. Born-Oppenheimer molecular dynamic (BOMD)[16] simulations were conducted at the B3LYP/6-31G(d) level for 100 picoseconds to access the kinetic stability. The stochastic search was realized using the

GXYZ program,[17] the CCSD(T) calculations were carried out using the MolPro 2012.1 package,[18] and all other calculations were performed using the Gaussian 09 package.[19]

Conflicts of interest

There are no conflicts to declare.

Acknowledgements

This project was supported by the NSFC (Grant No. 21720102006, 21273140, 21471092 and 21503252), the Special Program for Applied Research on Supercomputation of the NSFC-Guangdong Joint Fund (the second phase) (Grant No. U1501501), the Shanxi 1331KIRT, the Foundation of State Key Laboratory of Coal Conversion (Grant No. J17-18-610), the Program for the Outstanding Innovative Teams of Higher Learning Institutions of Shanxi Province, and the high performance computing platform of Shanxi University.

Notes and references

1 (*a*) R. Hoffmann, R. W. Alder and C. F. Wilcox, Jr., *J. Am. Chem. Soc.*, 1970, **92**, 4992; (*b*) J. B. Collins, J. D. Dill, E. D. Jemmis, Y. Apeloig, P. v. R. Schleyer, R. Seeger and J. A. Pople, *J. Am. Chem. Soc.*, 1976, **98**, 5419; (*c*) K. Sorger and P. v. R. Schleyer, *THEOCHEM*, 1995, **338**, 317; (*d*) D. Rottger and G. Erker, *Angew. Chem., Int. Ed. Engl.*, 1997, **36**, 812; (*e*) L. Radom and D. R. Rasmussen, *Pure Appl. Chem.*, 1998, **70**, 1977; (*f*) W. Siebert and A. Gunale, *Chem. Soc. Rev.*, 1999, **28**, 367; (*g*) R. Keese, *Chem. Rev.*, 2006, **106**, 4787; (*h*) G. Merino, M. A. Mendez-Rojas, A. Vela and T. Heine, *J. Comput. Chem.*, 2007, **28**, 362; (*i*) L. M. Yang, E. Ganz, Z. F. Chen, Z. X. Wang and P. v. R. Schleyer, *Angew. Chem., Int. Ed.*, 2015, **54**, 9468.
2 (*a*) K. Exner and P. v. R. Schleyer, *Science*, 2000, **290**, 1937; (*b*) Z. X. Wang and P. v. R. Schleyer, *Science*, 2001, **292**, 2465.
3 V. Vassilev-Galindo, S. Pan, K. J. Donald and G. Merino, *Nat. Rev. Chem.*, 2018, **2**, 0114.
4 X. Li, L. S. Wang, A. I. Boldyrev and J. Simons, *J. Am. Chem. Soc.*, 1999, **121**, 6033.
5 X. Li, H. F. Zhang, L. S. Wang, G. D. Geske and A. I. Boldyrev, *Angew. Chem., Int. Ed.*, 2000, **39**, 3630.
6 L. S. Wang, A. I. Boldyrev, X. Li and J. Simons, *J. Am. Chem. Soc.*, 2000, **122**, 7681.
7 (*a*) C. Romanescu, T. R. Galeev, W. L. Li, A. I. Boldyrev and L. S. Wang, *Acc. Chem. Res.*, 2013, **46**, 350; (*b*) C. Romanescu, T. R. Galeev, W. L. Li, A. I. Boldyrev and L. S. Wang, *Angew. Chem., Int. Ed.*, 2011, **50**, 9334; (*c*) W.-L. Li, C. Romanescu, T. R. Galeev, Z. A. Piazza, A. I. Boldyrev and L.-S. Wang, *J. Am. Chem. Soc.*, 2012, **134**, 165; (*d*) T. R. Galeev, C. Romanescu, W. L. Li, L. S. Wang and A. I. Boldyrev, *Angew. Chem., Int. Ed.*, 2012, **51**, 2101.
8 (*a*) Y. Pei, W. An, K. Ito, P. v. R. Schleyer and X. C. Zeng, *J. Am. Chem. Soc.*, 2008, **130**, 10394; (*b*) X. Y. Zhang and Y. H. Ding, *Comput. Theor. Chem.*, 2014, **1048**, 18; (*c*) J. O. C. Jimenez-Halla, Y. B. Wu, Z. X. Wang, R. Islas, T. Heine and G. Merino, *Chem. Commun.*, 2010, **46**, 8776; (*d*) Y. B. Wu, Y. Duan, H. G. Lu and S. D. Li, *J. Phys. Chem. A*, 2012, **116**, 3290; (*e*) A. C. Castro, G. Martinez-Guajardo, T. Johnson, J. M. Ugalde, Y.-B. Wu, J. M. Mercero, T. Heine, K. J. Donald and G. Merino, *Phys. Chem. Chem. Phys.*, 2012, **14**, 14964; (*f*) R. Grande-Aztatzi, J. L. Cabellos, R. Islas, I. Infante, J. M. Mercero, A. Restrepo and G. Merino, *Phys. Chem. Chem. Phys.*, 2015, **17**, 4620; (*g*) J. C. Guo, G. M. Ren, C. Q. Miao, W. J. Tian, Y. B. Wu and X. T. Wang, *J. Phys. Chem. A*, 2015, **119**, 13101; (*h*) J. C. Guo, L. Y. Feng, X.-Y. Zhang and H. J. Zhai, *J. Phys. Chem. A*, 2018, **122**, 1138; (*i*) J. C. Guo, W. J. Tian, Y. J. Wang, X. F. Zhao, Y. B. Wu, H. J. Zhai and S. D. Li, *J. Chem. Phys.*, 2016, **144**, 244303; (*j*) Z. H. Cui, J. J. Sui and Y. H. Ding, *Phys. Chem. Chem. Phys.*, 2015, **17**, 32016; (*k*) Z. H. Cui, V. Vassilev-Galindo, J. L. Cabellos, E. Osorio, M. Orozco, S. Pan, Y. H. Ding and G. Merino, *Chem. Commun.*, 2017, **53**, 138.
9 (*a*) Y. B. Wu, H. G. Lu, S. D. Li and Z. X. Wang, *J. Phys. Chem. A*, 2009, **113**, 3395; (*b*) Y. B. Wu, J. L. Jiang, R. W. Zhang and Z. X. Wang, *Chem. – Eur. J.*, 2010, **16**, 1271; (*c*) Y. B. Wu, Y. Q. Li, H. Bai, H. G. Lu, S. D. Li, H. J. Zhai and Z. X. Wang, *J. Chem. Phys.*, 2014, **140**, 104302; (*d*) Y.-B. Wu, Y. Duan, G. Lu, H.-G. Lu, P. Yang, P. v. R. Schleyer, G. Merino, R. Islas and Z.-X. Wang, *Phys. Chem. Chem. Phys.*, 2012, **14**, 14760; (*e*) Y. B. Wu, J. L. Jiang, H. G. Lu, Z. X. Wang, N. Perez-Peralta, R. Islas, M. Contreras, G. Merino, J. I. C. Wu and P. v. R. Schleyer, *Chem. – Eur. J.*, 2011, **17**, 714.
10 (*a*) M. Saunders, *J. Comput. Chem.*, 2004, **25**, 621; (*b*) P. P. Bera, K. W. Sattelmeyer, M. Saunders, H. F. Schaefer and P. v. R. Schleyer, *J. Phys. Chem. A*, 2006, **110**, 4287.
11 (*a*) D. Y. Zubarev and A. I. Boldyrev, *J. Org. Chem.*, 2008, **73**, 9251; (*b*) D. Y. Zubarev and A. I. Boldyrev, *Phys. Chem. Chem. Phys.*, 2008, **10**, 5207.
12 B. Cordero, V. Gomez, A. E. Platero-Prats, M. Reves, J. Echeverria, E. Cremades, F. Barragan and S. Alvarez, *Dalton Trans.*, 2008, 2832.
13 A. E. Reed, L. A. Curtiss and F. Weinhold, *Chem. Rev.*, 1988, **88**, 899.
14 (*a*) P. v. R. Schleyer, C. Maerker, A. Dransfeld, H.-J. Jiao and N. J. R. E. Hommes, *J. Am. Chem. Soc.*, 1996, **118**, 6317; (*b*) Z. F. Chen, C. S. Wannere, C. Corminboeuf, R. Puchta and P. v. R. Schleyer, *Chem. Rev.*, 2005, **105**, 3842.
15 P. v. R. Schleyer, H. J. Jiao, M. N. Glukhovtsev, J. Chandrasekhar and E. Kraka, *J. Am. Chem. Soc.*, 1994, **116**, 10129.
16 (*a*) V. Bakken, J. M. Millam and H. B. Schlegel, *J. Chem. Phys.*, 1999, **111**, 8773; (*b*) X. S. Li, J. M. Millam and H. B. Schlegel, *J. Chem. Phys.*, 2000, **113**, 10062.
17 H. G. Lu and Y. B. Wu, *GXYZ 2.0*, Shanxi University, Taiyuan, Shanxi, 2015.
18 H.-J. Werner, P. J. Knowles, G. Knizia, F. R. Manby, M. Schutz, P. Celani, T. Korona, R. Lindh, A. Mitrushenkov, G. Rauhut, K. R. Shamasundar, T. B. Adler, R. D. Amos, A. Bernhardsson, A. Berning, D. L. Cooper, M. J. O. Deegan, A. J. Dobbyn,

F. Eckert, E. Goll, C. Hampel, A. Hesselmann, G. Hetzer, T. Hrenar, G. Jansen, C. Koppl, Y. Liu, A. W. Lloyd, R. A. Mata, A. J. May, S. J. McNicholas, W. Meyer, M. E. Mura, A. Nicklass, D. P. O'Neill, P. Palmieri, D. Peng, K. Pfluger, R. Pitzer, M. Reiher, T. Shiozaki, H. Stoll, A. J. Stone, R. Tarroni, T. Thorsteinsson and M. Wang, *MolPro 2012.1*, University College Cardiff Consultants Limited, Cardiff U.K., 2012.
19 M. J. Frisch, G. W. Trucks, H. B. Schlegel, G. E. Scuseria, M. A. Robb, J. R. Cheeseman, G. Scalmani, V. Barone, B. Mennucci, G. A. Petersson, H. Nakatsuji, M. Caricato, X. Li, H. P. Hratchian, A. F. Izmaylov, J. Bloino, G. Zheng, J. L. Sonnenberg, M. Hada, M. Ehara, K. Toyota, R. Fukuda, J. Hasegawa, M. Ishida, T. Nakajima, Y. Honda, O. Kitao, H. Nakai, T. Vreven, J. J. A. Montgomery, J. E. Peralta, F. Ogliaro, M. Bearpark, J. J. Heyd, E. Brothers, K. N. Kudin, V. N. Staroverov, R. Kobayashi, J. Normand, K. Raghavachari, A. Rendell, J. C. Burant, S. S. Iyengar, J. Tomasi, M. Cossi, N. Rega, J. M. Millam, M. Klene, J. E. Knox, J. B. Cross, V. Bakken, C. Adamo, J. Jaramillo, R. Gomperts, R. E. Stratmann, O. Yazyev, A. J. Austin, R. Cammi, C. Pomelli, J. W. Ochterski, R. L. Martin, K. Morokuma, V. G. Zakrzewski, G. A. Voth, P. Salvador, J. J. Dannenberg, S. Dapprich, A. D. Daniels, O. Farkas, J. B. Foresman, J. V. Ortiz, J. Cioslowski and D. J. Fox, *Gaussian 09 Revision D.01*, Gaussian Inc., Wallingford CT, 2013.